inter noise
2013 | INNSBRUCK | AUSTRIA
15.-18. SEPTEMBER 2013
NOISE CONTROL FOR QUALITY OF LIFE

Vibro-acoustic responses of cylindrical shells with cardboard liners and determination of damping mechanisms

Hasan Koruk[1, a, b], Jason T. Dreyer[2, a], and Rajendra Singh[3, a]

[a] Acoustics and Dynamics Laboratory, NSF Smart Vehicle Concepts Center, Department of Mechanical and Aerospace Engineering, The Ohio State University, Columbus, Ohio 43210, USA

[b] Istanbul Technical University, Mechanical Engineering Department, 34437 Istanbul, Turkey

ABSTRACT

Cardboard liners are often installed in automotive drive shafts to reduce radiated noise over a certain frequency range. However, the precise mechanisms that yield noise attenuation for some modes are not well understood. To overcome this void, a thin shell (under free boundaries) with different cardboard liner thicknesses is examined using analytical, computational and experimental methods. Acoustic and vibration type frequency response functions are measured in an anechoic room, and the natural frequencies and the loss factors of structures are determined using several frequency response based methods and measured data. The adverse effects caused by closely spaced modes during the identification of modal loss factors are minimized. Finally, the modal loss factors of cylindrical shells with cardboard liners are estimated using several methods, and the sources of damping mechanisms are identified. The proposed procedure can be effectively used to model damped cylindrical shells (with cardboard liners) to predict their modal behavior and radiated noise.
Keywords: Experimental methods, damping mechanism, automotive noise control

1. INTRODUCTION

Cardboard liners are often installed in automotive drive shafts to control the structureborne and radiated noise over a certain frequency range. Although there are numerous articles on homogenous and undamped cylindrical shells [1-4], the precise cardboard liner mechanisms that yield noise attenuation for certain modes of a cylindrical shell are not well understood. In fact, no prior study has analytically examined the vibro-acoustics of cylindrical shells with cardboard liners though attempts have been made to simulate the cardboard liner as a distributed mass element in large scale computational models [5]. Although a few accelerance frequency response functions, with and without cardboard liners, have been measured [6-9], modal parameters of such structures, including their damping levels, have not been quantified in a systematic way. Overall, the effect of cardboard thickness has not been studied, and their damping mechanisms have not been explored in the literature [6-9]. This article attempts to fill this void with a controlled experimental study and by analytically or computationally examining certain shell vibration modes and damping mechanisms.

1 koruk@itu.edu.tr
2 dreyer.24@osu.edu
3 singh.3@osu.edu

2. PROBLEM FORMULATION

The following approximate solutions for the natural frequencies of a cylindrical shell are utilized to design the experiment and select the nominal dimensions of a tube such as the length (*l*), thickness (*h*) and radius (*R*). The natural frequency, ω_{mn} (rad/s) for mode (*m*,*n*) of a homogeneous cylindrical shell, can be approximated from the following frequency equation that is based on the classical Love's equation [1] and an infinite shell model [2]:

$$\begin{vmatrix} K\left(k_z^2+\frac{1-\mu}{2}k_\theta^2\right)-\rho h\omega^2 & \frac{K(1+\mu)}{2}k_z k_\theta & \frac{K\mu}{R}k_z \\ \frac{K(1+\mu)}{2}k_z k_\theta & \left(K+\frac{D}{R^2}\right)\left(k^2-\frac{1+\mu}{2}k_z^2\right)-\rho h\omega^2 & \left(\frac{K}{R}k_\theta+\frac{D}{R}k^2 k_\theta\right) \\ \frac{K\mu}{R}k_z & \left(\frac{K}{R}k_\theta+\frac{D}{R}k^2 k_\theta\right) & Dk^4+\frac{K}{R^2}-\rho h\omega^2 \end{vmatrix}=0 \quad (1)$$

Here *m* and *n* are axial and circumferential modal indices, respectively; *R* and *h* are the radius and thickness of a cylinder, respectively; $k_\theta = n/R$ is the wave number in the circumferential direction, k_z is the modal number in the axial direction and $k=\sqrt{k_z^2+k_\theta^2}$ is the structural wave number; $K = Eh/(1-\mu)$ is the membrane stiffness of the shell, and $D = Eh^3/\left[12(1-\mu^2)\right]$ is the bending stiffness of the shell where μ is the Poisson's ratio, *E* is the Young's modulus and ρ is the mass density. The modal wave number in the axial (*z*) direction under free-free boundary conditions is given by $k_{zm} = (m-0.5)\pi/l$ for $m \ge 2$ where *l* is the length of the cylinder. Note that the beam functions cannot provide a solution for $m=0$ and $m=1$. Accordingly, analytical expressions for ω_{0n} and ω_{1n} (in rad/s) for $m=0$ and $m=1$ modes are determined by using

$$\omega_{0n}^2 = \frac{E}{\rho}\frac{h^2}{12R^4}\frac{n^2\left(n^2-1\right)^2}{n^2+1} \quad (2)$$

$$\omega_{1n}^2 = \omega_{0n}^2\left(n^2+1\right)\frac{n^2 l^2 + 24(1-\mu)R^2}{12R^2+n^2\left(n^2+1\right)l^2} \quad (3)$$

Figure 1 illustrates the example case of a cylindrical shell with a cardboard liner; sensors used for experimental study are also shown. The boundary conditions at x = 0 and *l* are assumed to be free. Preliminary experiments performed on shells with typical cardboard liners show that it is difficult to determine modal parameters, especially the modal loss factors when the structure is highly damped. Accordingly, several cardboard samples of increasing thickness (h_2) are prepared. Furthermore, results with a different thickness (h_2) should provide a better understanding of the modes and sources of damping. Specifically, the shell thickness (h_1), outer diameter (*d*) and length (*l*) are determined to be 2.1, 152.4 and 457.2 mm, respectively, while three cardboard liners are prepared with h_2 = 0.31, 0.62 and 0.98 mm. The outer diameter of the cardboard is equal to the inner diameter of the base (aluminium) tube, and thus an interference fit describes the assembled structure. The mass density (ρ) of the aluminium tube is 2704 kg/m^3 while the cardboard density is determined to be 649 kg/m^3. Young's modulus and Poisson's ratio of the base aluminium tube are 71.0 GPa and 0.33, respectively.

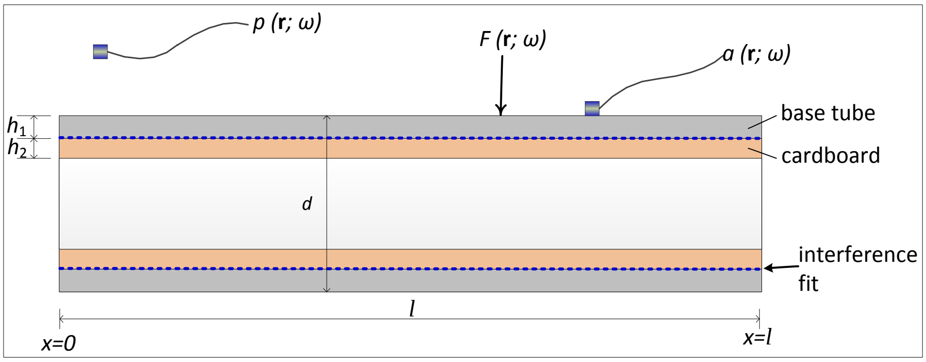

Figure 1 – Example case: An aluminium cylindrical shell with a cardboard liner; measurements include sound pressure (p), structure acceleration (a) and excitation force (F)

Both vibration $\tilde{A}_{ij}(\omega)=\tilde{a}_i(\omega)/\tilde{F}_j(\omega)$ and acoustic $\tilde{G}_{ij}(\omega)=\tilde{p}_i(\omega)/\tilde{F}_j(\omega)$ type frequency response functions are measured on samples with different cardboard liners in an anechoic room where 'a' is the acceleration, 'p' is the sound pressure and 'F' is the excitation force; i and j are the response and excitation point indices, respectively; and ω is the excitation frequency. Overall, the main objectives of this study are as follows: 1. Design a controlled vibro-acoustic experiment to measure $\tilde{A}_{ij}(\omega)$ and $\tilde{G}_{ij}(\omega)$ on a cylindrical shell with several cardboard liners; 2. Determine the first ten natural frequencies and modes of a cylindrical shell without and with the cardboard liners (up to 1950 Hz); and 3. Estimate the loss factors of first 5 modes, and identify possible sources of damping.

3. VIBRO-ACOUSTIC EXPERIMENTS

Before conducting detailed $\tilde{A}_{ij}(\omega)$ and $\tilde{G}_{ij}(\omega)$ measurements, the proper locations of excitation, accelerometer and microphone and the suspension method [10-12] are identified using a finite element model of an untreated cylindrical shell. Preliminary $\tilde{A}_{ij}(\omega)$ and $\tilde{G}_{ij}(\omega)$ measurements are performed to select the best signal processing parameters. For instance, $\tilde{A}_{ij}(\omega)$ measurements are obtained with a frequency resolution of 0.078, 0.125 and 0.25 Hz while $\tilde{G}_{ij}(\omega)$ measurements are performed with 0.063 and 0.125 Hz resolution. Measured data with a finer frequency resolution is used to identify the damping at the lower modes. Also, the autospectra of the force signal are examined to ensure that the structure is properly excited over the frequency range of interest. Each power spectrum is found using 5 averages. Sample $\tilde{A}_{ij}(\omega)$ of Figure 2 shows that the coherence is nearly at unity except at anti-resonances and beyond 1950 Hz.

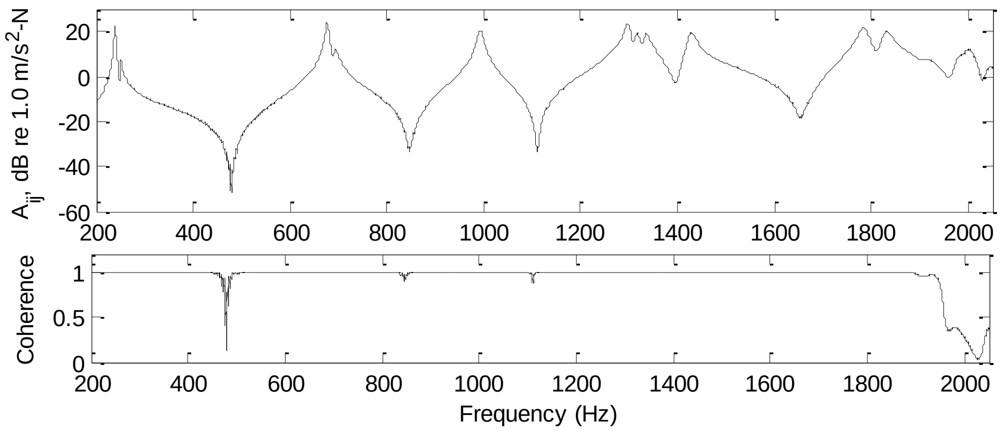

Figure 2 – Typical $\tilde{A}_{ij}(\omega)$ measurement on a treated cylindrical shell with h_2 = 0.62 mm liner and its coherence function

Since the mass loading effect of an accelerometer leads to a shift in the frequencies, the natural frequencies of the shell structure are determined by using acoustic pressure to force transfer functions $\tilde{G}_{ij}(\omega)$. Nevertheless, modal loss factors are estimated using accelerances $\tilde{A}_{ij}(\omega)$ data and half-power, line-fit and circle-fit methods [10]. Also, a very fine frequency resolution is employed for better accuracy and for a clear recognition of symmetrical mode pairs. The measurement period is selected to be sufficiently long to ensure that the signal approaches zero at the end of its minimal period. Consequently, there is no need to apply a particular windowing function; hence, there is minimal uncertainty in the identified modal loss factors due to the choice of window function. Also, experiments are performed only under free-free boundary conditions to eliminate any uncertainty due to boundary damping and stiffness. Overall, the first ten shell modes of structures are successfully identified.

4. COMPARISON OF NATURAL FREQUENCIES

The natural frequencies of the homogenous shell are first calculated using approximate analytical formulas given by Equations (1-3). Then, the Abaqus finite element program [13] is utilized for the computational modal analysis with 8554 (S4R) elements. Table 1 compares the experimental, analytical and computational natural frequencies of a homogeneous cylindrical shell. The symmetrical mode pairs are identified for both untreated and treated samples with h_2 = 0.31 and 0.62 mm liners though the symmetrical modes disappear when the h_2 = 0.98 mm liner is employed due to damping effect. It is seen that the error is less than 1% for the computational method but higher errors (say up to 6%) are seen for the analytical method. The average errors are about 0.4 and 4.4% for the computational and approximate analytical methods, respectively. Error in the analytical natural frequencies is due to the simplifying assumptions made in the shell vibration formulation [2], especially for the (0,*n*) and (1,*n*) modes.

Table 1 – Comparison of natural frequencies (ω_{mn}) of a homogeneous base cylinder (Aluminium material, l = 457.2 mm, d = 152.4 mm and h_1 = 2.1 mm)

Mode		Experimental	Analytical	Computational
Index	(*m*,*n*)	ω_{mn} (Hz)		
1	(0,2)	247.0, 248.4	234.9	248.7
2	(1,2)	258.6, 259.9	245.4	258.9
3	(0,3)	699.4, 701.9	664.5	704.6
4	(1,3)	714.3, 716.0	679.1	717.8
5	(2,3)	1023.4, 1025.8	988.2	1017.8
6	(2,2)	1339.3, 1343.8	1284.7	1348.2
7	(0,4)	1353.9, 1358.3	1274.0	1354.1
8	(1,4)	1365.6, 1372.1	1290.5	1368.0
9	(2,4)	1472.4, 1476.0	1451.0	1481.9
10	(3,4)	1834.6, 1841.8	1791.6	1840.8

Measured natural frequencies of the treated shell samples with different cardboard liners of thickness h_2 are given in Table 2. The natural frequencies of the treated shells decrease at all modes as h_2 is increased. The overall reductions are about 1.6%, 3.2% and 4.2% for the treated cylinders with h_2 = 0.32, 0.62 and 0.98 mm, respectively.

Table 2 – Measured natural frequencies (ω_{mn}) of the treated shell structures with three cardboard liners. Refer to Table 1 for the natural frequencies of the base (untreated) cylinder.

Mode		h_2 = 0.31 mm	h_2 = 0.62 mm	h_2 = 0.98 mm
Index	(m,n)	ω_{mn} (Hz)		
1	(0,2)	243.2, 244.5	238.6, 240.0	236.3
2	(1,2)	254.3, 255.7	249.5, 250.8	246.8
3	(0,3)	688.2, 691.0	675.3, 678.5	672.8
4	(1,3)	702.7, 704.6	689.7, 692.1	686.5
5	(2,3)	1007.5, 1010.4	990.8, 995.8	983.8
6	(2,2)	1317.6, 1322.3	1297.1, 1300.2	1286.8
7	(0,4)	1332.1, 1336.3	1312.0, 1316.0	1301.5
8	(1,4)	1345.4, 1352.1	1326.0, 1336.0	1314.0
9	(2,4)	1450.3, 1453.1	1419.0, 1427.0	1414.0
10	(3,4)	1808.0, 1812.7	1776.0, 1783.5	1762.4

5. EXTRACTION OF MODAL LOSS FACTORS

Since it is virtually impossible to have a perfectly symmetrical shell, closely spaced peaks are found at each mode in measured accelerances $\tilde{A}_{ij}(\omega)$. Also, some resonant peaks may contain more than one mode. The adverse effects of such closely-spaced modes encountered during the identification process are minimized via the line-fit or circle-fit type methods [10] that take into account both accelerance $\tilde{A}_{ij}(\omega)$ amplitude and phase data when distinct modes are well-excited; these methods are used in addition to the conventional half-power method [10]. Overall, the averaged modal loss factors (η_{mn}) of untreated and treated samples are compared in Table 3. Observe that the loss factors are about 0.4, 0.7 and 1.2% for the treated cylindrical shells with h_2 = 0.31, 0.62 and 0.98 mm, respectively. Note that the symmetrical modes at a higher frequency with h_2 = 0.98 mm could not be separated, and thus no results are given for such modes.

Table 3 – Modal loss factors of the untreated and treated cylindrical shells. Refer to Table 2 for natural frequencies.

Mode		h_2 = 0 mm	h_2 = 0.31 mm	h_2 = 0.62 mm	h_2 = 0.98 mm
Index	(m,n)	η_{mn} (%)			
1	(0,2)	0.130	0.514	0.651	1.192
2	(1,2)	0.114	0.434	0.693	1.093
3	(0,3)	0.068	0.364	0.668	1.252
4	(1,3)	0.055	0.392	0.716	*
5	(2,3)	0.073	0.357	0.638	*

* could not be identified

6. ESTIMATION OF DAMPING MECHANISMS

The Ross-Kerwin-Ungar equations [14] are used to predict the equivalent elastic and damping properties of a composite structure assuming that the cardboard liner acts as a free-layer damping treatment. It is assumed that the cardboard liner follows the deformation of the base tube and the interfacial damping mechanism is ignored. As a result, the averaged loss factors of the treated cylindrical shells with h_2 = 0.31, 0.62 and 0.98 mm are found to be 0.23, 0.41 and 0.68%, respectively.

Next, a recently developed finite element formulation for composite structures [15] is used to model the cylindrical shells with cardboard liners. This formulation is based on a complex eigenvalue method, and it has been validated to predict modal behaviour of composite structures including their modal loss factors with high accuracy. This method yields averaged loss factors to be about 0.21, 0.37 and 0.59% for h_2 = 0.31, 0.62 mm and 0.98 mm, respectively.

The averaged loss factors (for the first 5 modes) are plotted as a function of the cardboard thickness in Figure 3. The values of loss factors predicted via analytical and computational approaches are very close to each other, though the measured loss factors are higher than theoretical results. Since both analytical and computational methods consider only material damping, the difference between measured (actual) and computational or analytical results (based on simplifying damping formulation) could be attributed to the friction damping. This is due to the interference fit in the assembly. The loss factors due to friction should increase as the cardboard thickness (and thus the normal load) is increased. Also, it is found that the ratios between the frictional and total system loss factors are 0.49, 0.46 and 0.50 for the treated cylinders with h_2 = 0.31, 0.62 and 0.98 mm, respectively.

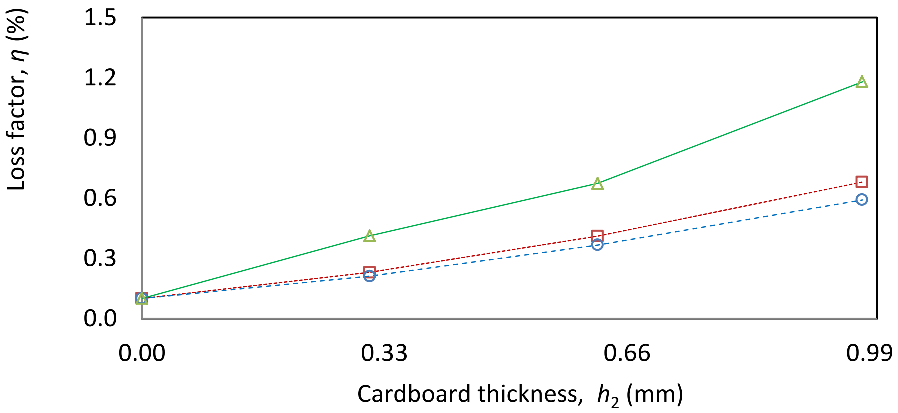

Figure 3 – Comparison of the averaged loss factors as a function of cardboard liner thickness

(Key: □ Analytical ○ Computational and Δ Experimental)

7. CONCLUSION

This article investigates the effect of cardboard liners on the resonant vibro-acoustic responses of cylindrical shells. A controlled experiment is designed to measure acoustic and vibration frequency response functions with different cardboard thicknesses in an anechoic room. The natural frequencies and loss factors of structures are determined using several frequency domain methods and measured data. The sources of damping mechanisms are identified. This suggests that the dry friction contributes to about half of the overall damping. More detailed results and models will be reported in a future article. The proposed procedure can be effectively used to model a damped cylindrical shell (with a cardboard liner) and to predict their vibration and radiated noise levels.

ACKNOWLEDGEMENTS

We acknowledge the Smart Vehicle Concepts Center (www.SmartVehicleCenter.org) and the National Science Foundation Industry/University Cooperative Research Centers program (www.nsf.gov/eng/iip/iucrc) for supporting this fundamental study.

REFERENCES

[1] Arthur W. Leissa, *Vibration of Shells* (Acoustical Society of America, USA, 1993).

[2] C. Wang, J. C. S. Lai, "Prediction of natural frequencies of finite length circular cylindrical shells," Appl. Acoust., 59, 385-400 (2000).

[3] C. Wang, J. C. S. Lai, "The sound radiation efficiency of finite length acoustically thick circular cylindrical shells under mechanical excitation I: Theoretical analysis," J. Sound Vib., 232(2), 431-447 (2000).

[4] C. Wang and J. C. S. Lai, "The sound radiation efficiency of finite length circular cylindrical shells under mechanical excitation II: Limitations of the infinite length model," J. Sound Vib., 241(5), 825-838 (2001).
[5] N. Y. Wani, V. K. Singh, G. Falbo and V. D. Monkaba, "Finite element model correlation of an automotive propshaft with internal and external dampers," SAE Paper no. 2004-01-0862, 2004.
[6] M. G. Foulkes, J. P. De Clerck and R. Singh, "Vibration characteristics of cardboard inserts in shells," SAE Transactions Journal of Passenger Cars: Mechanical Systems, 112(6), 1718-1725 (2004).
[7] M. Moetakef, A. Bresky, M. Zilberman, T. Pham, R. Egenolf and B. Bonhard, "Reducing high frequency driveshaft radiated noise by polymer liners," SAE Paper no. 2005-01-3554, 2005.
[8] S. Theodossiades, H. Rahnejat and P. Kelly, "On the effect of cardboard liners on impact-induced high frequency vehicular driveline vibrations," Proc. IDETC/CIE 2007, Paper no. DETC2007-35692 (2007).
[9] Z. Sun, D. Schankin, W. Braun and J. Ley, "Attenuation of driveline vibrations through tuning of propeller shaft liners," SAE Paper no. 2011-01-1547, 2011.
[10] David J. Ewins, *Modal Testing: Theory, Practice and Application* (Research Studies Press, 2nd Edition, England, 2000).
[11] FINES, Finite Element for Structures, Istanbul Technical University, Turkey, 2006.
[12] ICATS, Imperial College Testing Analysis and Software, Imperial Collage, England, 2006.
[13] ABAQUS 6.9.1., Finite Element Software, 2010.
[14] Ahid D. Nashif, David I. G. Jones and John P. Henderson, *Vibration Damping* (John Wiley & Sons, New York, USA, 1985).
[15] K. Y. Sanliturk and H. Koruk, "Development and validation of a composite finite element with damping capability," Compos. Struct., 97, 136-146 (2013).